Banded Spherulites in PS−PLLA Chiral Block Copolymers

Chia-Cheng Chao,[‡] Chun-Ku Chen,[†] Yeo-Wan Chiang,[†] and Rong-Ming Ho*[,†,‡]

Department of Chemical Engineering, National Tsing Hua University, Hsinchu 30013, Taiwan, R.O.C., and Institute of Nanoengineering and Microsystems, National Tsing Hua University, Hsinchu 30013, Taiwan, R.O.C

Received October 31, 2007; Revised Manuscript Received March 10, 2008

ABSTRACT: In this study, thin-film samples of semicrystalline block copolymer (BCP), polystyrene-*b*-poly(L-lactide) (PS−PLLA), were prepared by solution-casting from dichloromethane solution (1 wt % of PS−PLLA). As observed by polarized light microscopy (PLM), banded spherulites can be found in the PS−PLLA thin-film samples crystallized from melt. By contrast, no banded spherulites can be obtained in crystallized PLLA homopolymer under similar crystallization conditions. However, the formation of banded spherulites for PLLA homopolymer can be achieved by blending compatible poly(ε-caprolactone) (PCL) homopolymer. Also, blends of PS−PLLA and poly(D-lactide) (PDLA) were prepared; no banded spherulites can be obtained in crystallized blends having equimolar PLLA and PDLA (namely, racemic blends). As a result, we suggest that the effect of chirality on polylactide crystallization is necessary for the induction of cooperative lamellar twisting along the radial growth direction to form banded spherulites. Moreover, the chiral effect might be enhanced by the introduction of diluents, such as compatible PCL homopolymer that promotes the formation of banded spherulites; this is referred to the effect of diluents. In contrast to the PLLA/PCL blends, a significant decrease in the band spacing of PS−PLLA banded spherulites (namely, the increase in twisting power) can be found. We speculate that the incompatible PS block chemically jointed with the PLLA block may intensify the effect of diluents so as to increase the imbalanced stress at crystalline lamellar fold surfaces for lamellar twisting. The morphological evolution of the banded spherulites was further investigated by using transmission electron microscopy and field-emission scanning electron microscopy. A hypothetic model was thus proposed to reveal the mechanism for the formation of curved crystalline lamellae in crystallized polylactide BCP.

Introduction

A banded spherulite (i.e., the presence of concentric rings or extinction bands in PLM) is a common morphological feature in crystalline polymers.[1–4] It is generally believed that the formation of the banded spherulite is attributed to lamellar twisting along the radial growth direction.[5–10] Various mechanisms of the lamellar twisting have been proposed.[5–7,11–19] Periodically spaced lamellar twisting in spherulites results from equally spaced screw dislocations along the growth direction of lamellae. The overall twisting is thus initiated by the sequence of transverse screw dislocation with the same sign so as to generate extinction bands in PLM. Also, a continuous twisting for the growth of crystalline lamellae might be conducted without the occurrence of screw dislocations for the development of extinction bands. The imbalanced stress at lamellar fold surfaces is usually regarded as the cause of the lamellar twisting. The staggering of chain folding might cause the chain stems to be nonorthogonal to the fold surfaces so as to generate unequal stresses at opposite fold surfaces which yield bending moment upon crystalline lamellae and finally results in the lamellar twisting.

The formation of the banded spherulites can be found in different crystalline polymeric materials. Among them, chiral polymers are frequently crystallized as twist lamellae so as to form the banded spherulites. The lamellar twisting is usually attributed to the effect of chirality on crystallization.[3,4,19–24] For instance, morphological textures with helical sense (that is, twist lamellar crystals) can be obtained from a series of chiral polyesters [PET(R*-n)] synthesized from (*R*)-(−)-4′-{ω-[2-(*p*-hydroxy-*o*-nitrophenyloxy)-1-propyloxy]-1-nonyloxy}-4-biphenylcarboxylic acid.[21,22] Also, the banded spherulites can be found in chiral poly(3-hydroxybutyrate-*co*-3-hydroxyhexanoate) (PHB-*co*-HHx), and the lamellar twisting indeed occurs during crystalline growth as evidenced by real-time AFM observation.[3] Recently, the crystallization of enantiomeric polylactides has been found to give curved crystalline lamellae with an exclusive direction at which the PLLA lamellae exhibited an S-shape texture whereas the PDLA lamellae appeared as a Z-shape texture.[25] However, the origins for the formation of twist lamellae to form the banded spherulites are still under debate.

Block copolymers (BCPs) consist of two or more chemically different polymeric chains covalently connected together so that the incompatibility of constituent blocks leads to a microphase separation and results in ordered nanostructures. In semicrystalline BCPs containing crystallizable block(s), the crystalline morphology is strongly dependent upon the experimental temperature, with respect to the order−disorder transition temperature (T_{ODT}), the crystallization temperature of the crystallizing block (T_c^c), and the glass transition of the amorphous block (T_g^a).[26–32] In other words, the crystalline morphology is the consequence of microphase separation, crystallization, and vitrification. Usually, a crystallization event dominates the morphological development while it occurs before a microphase separation (i.e., $T_c^c > T_{ODT} \gg T_g^a$), whereas the complicate crystallization process, such as confined crystallization, may perform while $T_{ODT} > T_c^c$. Consequently, the crystalline morphology is strongly determined by the crystallization temperature of the crystallizing block which also justifies the degree of vitrification in a confined environment. Namely, the dividing confined environments, i.e., hard confinement ($T_c^c < T_g^a$) and soft confinement ($T_c^c \geq T_g^a$), dictate the final morphology of crystallized BCPs. Also, the crystallization behavior under confinement is also dependent upon a confined geometry in addition to the confined environment.[32]

* To whom all correspondence should be addressed: Tel 886-3-5738349; Fax 886-3-5715408; e-mail rmho@mx.nthu.edu.tw.
[†] Department of Chemical Engineering.
[‡] Institute of Nanoengineering and Microsystems.

10.1021/ma702416n CCC: $40.75
Published on Web 05/07/2008

According to our previous studies on a semicrystalline BCP, polystyrene-*b*-poly(L-lactide) (PS−PLLA), interesting crystalline morphologies were observed. For symmetric PS−PLLA BCP, a microphase-separated lamellar nanostructure can be obtained from self-assembly, and the crystallization of the PLLA block can be carried out from a hard confinement (i.e., $T_{ODT} >$ the glass transition temperature of PS ($T_{g,PS}$) > the crystallization temperature of PLLA ($T_{c,PLLA}$)) to a soft confinement (i.e., $T_{ODT} > T_{c,PLLA} \geq T_{g,PS}$). While $T_{g,PS} > T_{c,PLLA}$, the ordered nanostructure can persevere due to the vitrified microdomains of the PS block. By contrast, if $T_{c,PLLA} \geq T_{g,PS}$, the crystallization may lead to the change on the microphase-separated nanostructure at which an undulated morphology was found. For PS−PLLA with PS-rich fraction, a novel microphase-separated nanostructure, a hexagonally packed helix, can be obtained from the self-assembly of PS−PLLA with volume fraction of PLLA (f_{PLLA}^{v}) ~0.35.[33] Furthermore, an interesting crystallized morphology can be observed; various crystalline PS−PLLA nanostructures were obtained by simply controlling $T_{c,PLLA}$ at which crystalline nanohelices (PLLA crystallization directed by helical confined microdomain) and crystalline cylinders (phase transformation of helical nanostructure dictated by crystallization) occur while $T_{g,PS} > T_{c,PLLA}$ and $T_{c,PLLA} \geq T_{g,PS}$, respectively.[34] For PS−PLLA with PLLA-rich fraction, a unique microphase-separated nanostructure, a hexagonally packed core−shell cylinder of which the PS microdomains appear as shells and PLLA microdomains appear as matrix and cores, can be found from the self-assembly of PS−PLLA with $f_{PLLA}^{v} \sim 0.65$.[35] The formation of those novel nanostructures—helix and core−shell cylinder—is attributed to the chiral effect on the self-assembly of BCPs so we named this PS−PLLA BCP as chiral BCP.[33,35]

In this study, we aim to investigate the crystalline morphologies for the PLLA-rich PS−PLLA possessing a core−shell cylinder nanostructure. Unlike the crystalline morphology in the microphase-separated lamellae or helix, microphase-separated nanostructure was ruined by crystallization in the PLLA-rich PS−PLLA. Furthermore, in contrast to the crystallization of polylactide homopolymers, we found that the banded spherulitic morphology can be much easily obtained in the PLLA-rich PS−PLLA. The presence of the PS block chemically jointed with the PLLA block is critical for the formation of the banded spherulites. Systematic studies are thus carried out to explore the origins for the formation of the banded spherulites in polylactides and their blends. To explore the significance of the chiral effect on polylactide crystallization, blends of PS−PLLA with poly(D-lactide) (PDLA) having equimolar PLLA and PDLA (namely, racemic blends) are prepared. Also, it is noted that the introduction of compatible diluents may promote the formation of the banded spherulites, and the effect is referred to the effect of diluents.[1] To examine the effect of diluents, blends of PLLA with compatible poly(ε-caprolactone) (PCL) are also prepared so that a systematic comparison between the banded spherulitic morphology in PLLA/PCL blends and PS−PLLA BCPs can be achieved. Consequently, the origins for the formation of the banded spherulites in chiral polymers are justified, and the corresponding mechanisms in the presence of chiral entities and diluents are proposed.

Experimental Section

Materials. The PS−PLLA BCP was prepared by using two-step living polymerization in sequence. The detailed synthetic routes were similar to our previous approach.[35] The molecular weights of PS and PLLA were 6000 and 13 900 g/mol, respectively. The PDI of the PS−PLLA was determined as 1.17. The volume fraction of the PLLA block was calculated as 0.65 by assuming the densities of PS and PLLA are 1.02 and 1.18 g/cm^3. Also, PLLA, PDLA, and PCL homopolymers were prepared by ring-opening polymerizations. The polymerization of the PLLA and PDLA homopolymers was performed by using $Sn(Oct)_2$ as catalyst and benzyl alcohol (BnOH) as initiator. The molecular weights of PLLA and PDLA were 12 800 and 11 800 g/mol, respectively, and the corresponding PDIs were 1.03 and 1.06, respectively. For the polymerization of PCL homopolymer, $[Al(EDBP)(\mu\text{-}OBn)]_2$ was used as initiator, and the molecular weight and PDI of the PCL were 2300 g/mol by ^{1}H NMR and 1.09, respectively. All the molecular weights were determined by ^{1}H NMR, and the PDIs were characterized by GPC.

Sample Preparation. Bulk samples of the BCPs were prepared by solution-casting from methylene chloride (CH_2Cl_2) solution (10 wt % of PS−PLLA) at room temperature for 1 week and then were placed under vacuum at 45 °C for 1 day to remove the residual solvent. Thin-film samples for PLM and FESEM was obtained by solution-casting from the CH_2Cl_2 solution (1 wt % of solute). Thin-film samples for TEM were obtained by spin-coating onto carbon-coated glass of the dilute solution. For isothermal crystallization experiments, the thin-film samples were quickly transferred from melt stage onto crystallization stage preset at desired temperature for crystallization.

Hydrolysis. It is known that aliphatic polyesters can be hydrolytically degraded because of the unstable character of the ester group.[36,37] Crystallized thin-film samples were placed in NaOH solution for 20 min to degenerate amorphous PLLA components and washed in MeOH solution. Those thin-film samples were then floated on water and picked by copper grid for TEM observation.

Blending. All blends were prepared by using the solution blending method. In PLLA/PCL blends, PLLA and PCL were dissolved in methylene chloride at a total concentration of 1 wt %, and then the solution was vigorously stirred for ~1 day. The volume fraction of PLLA homopolymer in the PLLA/PCL blends was 0.65. In the blends of PS−PLLA/PDLA, PS−PLLA and PDLA were also dissolved in methylene chloride at a total concentration of 1 wt %, and then the solution was vigorously stirred for ~1 day. In the blends of PS−PLLA/PDLA or PLLA/PDLA/PCL, the blends with equimolar PLLA and PDLA were prepared to form the racemic blends. The volume fraction of PCL homopolymer in the PLLA/PDLA/PCL blends was 0.35.

Differential Scanning Calorimetry (DSC). DSC experiments were carried out in a Perkin-Elmer DSC 7 with a controlled cooling system in a flowing N_2 atmosphere. The temperature and heat flow scales at specific scan rate were calibrated carefully with standard materials of cyclohexane and indium before experiment proceeds. The samples were first heated to 175 °C for 3 min in order to eliminate the crystalline residues and subsequently cooled at a rate of 150 °C/min to crystallization temperature, T_c, for isothermal crystallization processes. The DSC samples weight was around 5 mg for all measurements.

Polarized Light Microscopy (PLM). An Olympus BX-60 equipped with a hot stage was controlled by an INSTEC 200 central processor. A Carl-Zeiss Axiphot 2 equipped with a Mettler FP82 hot stage and a FP80 central processor was used. Both of them were carefully alignment before use and then were utilized to observe the thermal transitions and to analyze the optical textures. The hot stage was calibrated with standard materials within the precision of ±0.2 °C. To observe the melting of spherulites in PLLA, PLLA/PDLA, and PS−PLLA/PDLA blends, in-situ PLM was carried out at different temperatures (say 25, 170, 190, and 240 °C) and stayed for 10 min at each step.

Transmission Electron Microscopy (TEM). TEM experiments were carried out in a JEOL JEM-1200CXII at an accelerating voltage of 120 kV. The bright field transmission electron microscopy (TEM) images were obtained using the mass−thickness contrast from staining and shadowing. Staining was accomplished by exposing the samples to the vapor of a 4% aqueous RuO_4 solution for 3 h, and the locations with unsaturated bonds were bonding with RuO_4 to increase the mass−thickness contrast. A shadowing process has proven useful in contrast enhancement by the addition of heavy metal in a vacuum evaporator. The samples of carbon films were floated on water first and picked on copper grid and then shadowed by Pt/Pb = 4/1 30° tilted to the surface.

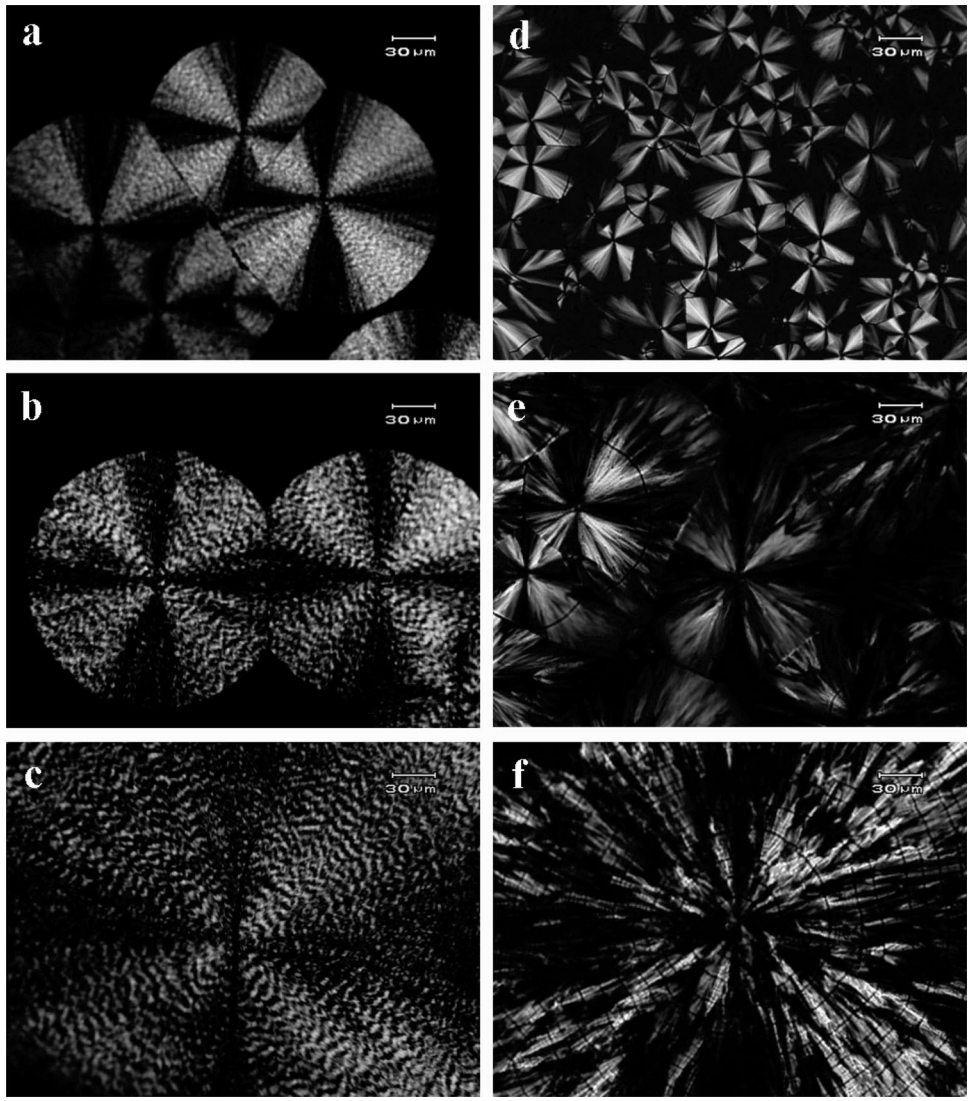

Figure 1. PLM morphologies of PS−PLLA banded spherulites (left) and PLLA spherulites (right) crystallized from melt at different temperatures: (a, d) at 110 °C; (b, e) at 120 °C; (c, f) at 135 °C.

Field-Emission Scanning Electron Microscopy (FESEM). FESEM observation was performed on a JEOL JSM-6700F using accelerating voltages of 1.5 keV. The crystalline lamellae of PS−PLLA thin-film samples were examined after hydrolysis. The samples were mounted to brass shims using carbon adhesive and then sputter-coated with 2−3 nm of platinum (the platinum coating thickness was estimated from a calculated deposition rate and experimental deposition time).

Results and Discussion

Crystallization of PS−PLLA. To examine the crystalline morphology of the PS−PLLA with PLLA-rich fraction synthesized in this study, thermal properties were examined by using DSC. The $T_{g,PLLA}$ was at ca. 53 °C and its $T_{m,PLLA}$ at 163 °C for the PS−PLLA samples quenched from melt, but the $T_{g,PS}$ was not measurable due to the occurrence of PLLA crystallization during heating. To resolve this problem, solution-casting samples were initially heated to 175 °C to erase thermal history and then rapidly cooled at 150 °C/min to 100 °C for 3 h so as to complete the PLLA crystallization. Subsequent DSC measurement was performed after complete crystallization; the $T_{g,PS}$ was at ca. 78 °C. The temperature of maximum crystallization rate was at ca. 100 °C, as determined from isothermal crystallization experiment. At high temperature (say 140 °C), no exothermic response can be recognized by DSC, indicating that crystallization cannot be proceeded at such high temperature. As a result, the crystallization window for the PLLA block in the PS−PLLA is approximately in the range of 55−130 °C. Furthermore, on the basis of the known interaction parameters of PS and PLA reported by Hillmyer,[38] $\chi(T) = 98.1/T - 0.112$, and assuming that the solubility parameters of PLA and PLLA are similar, the self-assembly of PS−PLLA should lead to strongly segregated microphase separation in the temperature range where PLLA crystallizes. As a result, a microphase-separated nanostructure, a hexagonally packed core−shell cylinder, was obtained after thermal annealing at the temperature above PLLA melting.[35] Nevertheless, the nanostructure was ruined by the PLLA crystallization while $T_{c,PLLA} > T_{g,PS}$, indicating that the crystallization process may govern the final morphology of self-assembled PS−PLLA even with strongly segregated microdomains. Consequently, an interesting crystalline morphology, banded spherulitic texture, was found.

Banded Spherulites of PS−PLLA. As observed by PLM (Figures 1a−c), a typical polymeric crystalline morphology (namely, spherulitic texture) can be found in PS−PLLA crystallized at different crystallization temperatures. Also, those spherulites exhibited concentric rings or extinction bands in PLM, namely, banded texture. By contrast, typical spherulites without extinction bands (Figure 1d–f) were found in PLLA

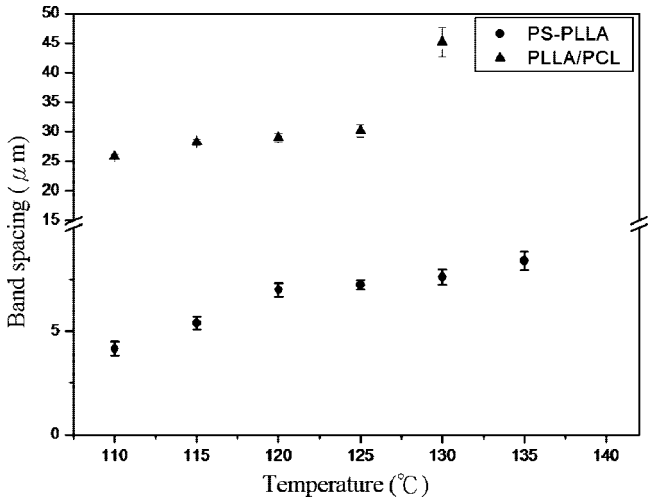

Figure 2. Crystallization temperature dependence of band spacing for the spherulites of PS−PLLA and PLLA/PCL blends.

homopolymer having molecular weight equal to PLLA block in the PS−PLLA studied. The size of the spherulite increased with the crystallization temperature in both the PLLA and PS−PLLA samples due to the decrease in nucleation density. Also, both samples exhibited Maltese cross textures and appeared as negative birefringence spherulites (i.e., the first and third quadrants of spherulite appear yellow but the second and fourth quadrants appear blue) with birefringence enhancement by gypsum plate. The appearance of the extinction bands is attributed to the direction of rotative optical axis (i.e., the direction of molecular chains) is parallel to the transmitted light of PLM. It is commonly believed that the formation of the banded spherulite is attributed to the crystalline lamellar twisting along the spherulitic radius during crystal growth. The lamellar twisting might be attributed to the formation of screw dislocations and/or continuous twisting for the growth of lamellae. Imbalanced stress at lamellar fold surfaces is usually regarded as the cause of the lamellar twisting so as to form helical ribbon-like texture that results in the banded spherulites. For chiral polymers, the effect of chirality for crystallization may lead to the imbalanced surface stresses. As a result, we speculate that the formation of the banded spherulites is dependent upon the effect of chirality (see below for details).

Furthermore, according to the average measurement on the periodicity of the extinction bands for at least 50 spherulites, the band spacing of the banded spherulites increased with the increase of crystallization temperature (Figure 2). The band spacing indeed corresponds to the half-pitch length of twist lamellae. Also, it is noted that the inversed value of the helical pitch length of twisting ribbons from self-assembly is defined as helical twisting power (HTP). The temperature dependence of the band spacing implicitly indicates that the cause of the lamellar twisting should be related to the crystal growth of the chiral polymers. It is also noted that the banded spherulites of PLLA homopolymer can only be obtained under specific crystallization process at which the PLLA was annealed at high temperature and then slowly cooled to preset temperature for isothermal crystallization.[24] Moreover, the band spacing in crystalline PLLA[24] is much larger than that in crystalline PS−PLLA studied here. Namely, a crystalline PS−PLLA possesses higher HTP for the formation of twist lamellae. So, the morphological results suggest that the banded spherulitic morphology can be easily obtained in the PS−PLLA as compared to the PLLA. In other words, the incompatible PS block chemically jointed with the PLLA block should play an important role in the formation of the banded spherulites in addition to the effect of chirality.

Crystalline Morphologies of PS−PLLA and PDLA Blends. The crystalline morphology of chiral polymers is inevitably affected by the chiral effect on crystalline asymmetry. Since the PLLA is a chiral polymer, blends of the PS−PLLA with poly(D-lactide) (PDLA) were prepared to examine the chiral effect on the formation of PLLA banded spherulites in PS−PLLA. It is known that racemic crystallites can be obtained by blending equimolar PLLA and PDLA due to the formation of PLLA/PDLA crystalline stereocomplex.[39,40] In contrast to the melting of polylactide homopolymers, a significant increase in melting temperature can be found in crystalline stereocomplex at which the melting is usually over 230 °C. In-situ PLM observation were carried out at high temperature for the identification of the crystalline stereocomplex (Figure 3). As observed, the formation of high-melting spherulites (that is crystalline stereocomplex) can be found in the blends of PS−PLLA/PDLA with equimolar PLLA and PDLA. Typical spherulitic morphology can be found in the blends of PS−PLLA/PDLA (Figures 4a−d). However, the banded texture cannot be found in the PS−PLLA/PDLA blends crystallized at different temperatures. In contrast to the formation of the banded spherulites in the PS−PLLA, the discrepancy in the spherulitic texture is explicitly attributed to the racemic character for the blends at which the Cotton effect in the circular dichroism spectrum becomes trivial (results no shown). It is obvious that the formation of the banded spherulites is strongly dependent upon the chiral effect on crystallization.

Banded Spherulites of Crystalline Polylactides and PCL Blends. In 1989, Keith and co-workers demonstrated that the morphological changes can be achieved by blending small concentration of compatible polymer diluents poly(vinyl butyral) (PVB) with PCL homopolymer.[1] The banded spherulites of crystalline PCL in blends is much more regular than that in neat PCL homopolymer, and the band spacing was found to decrease with the increase of the PVB fraction. In other words, the HTP increases with the introduction of PVB. Also, it is noted that the formation of such banded spherulites is referred to the lamellar twisting model. Because of the introduction of the non-crystallizable polymers, i.e., PVB, the tendency of the lamellar twisting is considerably enhanced by the noncrystallizable polymer that can act as diluents absorbed on crystal boundaries after PCL crystallization so as to cause the imbalance surface stress at crystalline lamellar fold surfaces. The enhancement is referred to the effect of diluents on the formation of the banded spherulites.

As observed, the formation of the banded spherulites can be found in the PS−PLLA but not in PLLA homopolymer under similar crystallization conditions. We speculate that the role of the PS block is similar to the compatible polymer diluents in the crystallization of the PS−PLLA by considering the compatibility induced by a chemical junction. First, we would like to know whether the effect of diluents does exist for the crystallization of the PLLA, and then a systematic comparison can be carried out to examine the hypothesis of the PS block as diluents for PLLA crystallization. To examine the effect of diluents on the crystallization of the PLLA, a compatible blending system, blends of PLLA and PCL homopolymers, was prepared in which the volume fraction of PLLA homopolymer in the PLLA/PCL blends is equal to the PLLA-rich PS−PLLA studied for the comparison (i.e., $f_{PLLA}^{v} = 0.65$). PLLA and PCL homopolymers are compatible in the melt state for low molecular weight components. Note that the molecular weights of PLLA and PCL in this study are low enough to ensure compatibility.[41,42] As shown in Figures 5a−d, the banded spherulites with negative birefringence character can be observed in the blends of PLLA

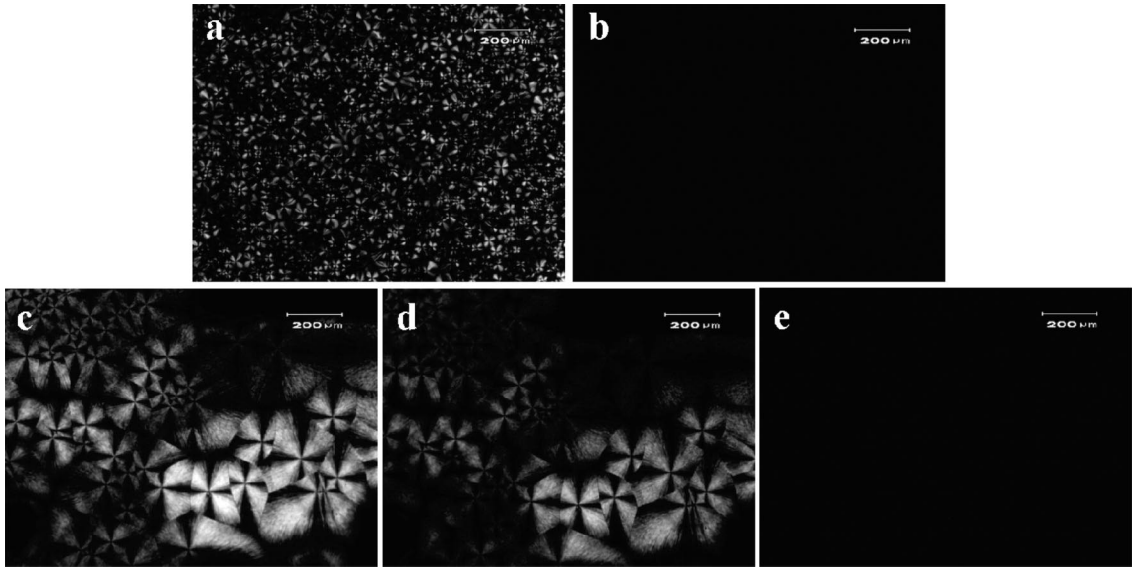

Figure 3. In-situ PLM spherulitic morphologies observed at different temperatures: PLLA homopolymer at (a) 25 °C; (b) 170 °C; PS−PLLA/PDLA blends with equimolar PLLA and PDLA at (c) 25 °C; (d) 190 °C; (e) 240 °C. The spherulites in the PLLA and blends are crystallized from melt at 120 and 160 °C, respectively.

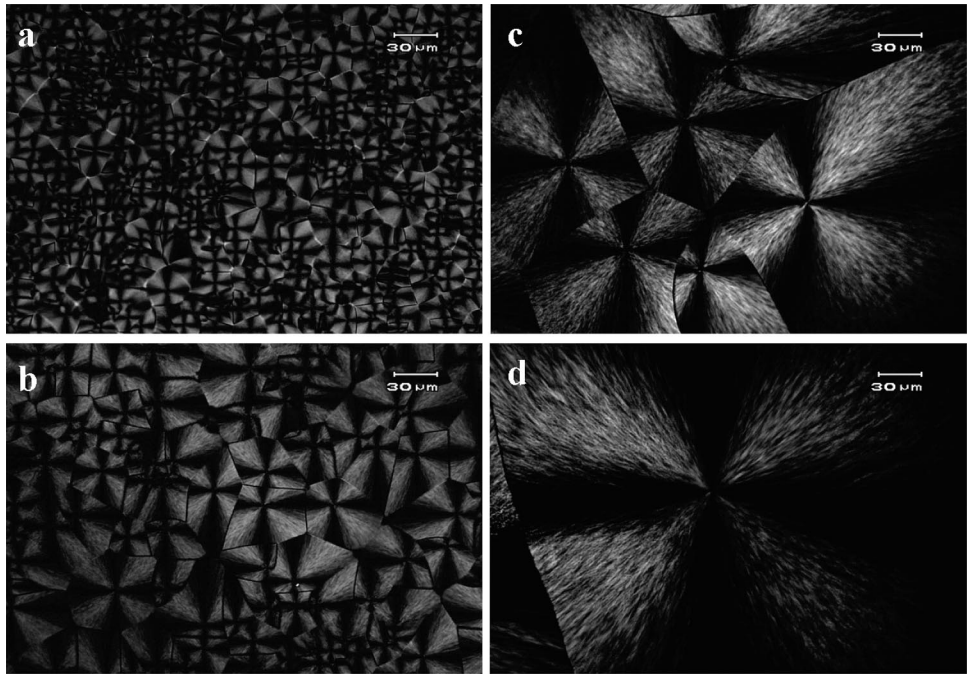

Figure 4. PLM morphologies of stereocomplex spherulites in the blends of PS−PLLA and PDLA with equimolar PLLA and PDLA crystallized from melt at different temperatures: (a) 130, (b) 140, (c) 150, and (d) 160 °C.

and PCL, and those spherulites appear much more regular banded texture as compared to that in the PS−PLLA. We speculate that the regularity in banded texture may result from the higher compatibility between PLLA and PCL homopolymers. The results are consistent with the effect of diluents on the formation of the banded spherulites even though the origin in the blends of PCL/PVB might be different than that in the blends of PLLA/PCL. As a result, we suggest that the effect of diluents is significant on the formation of the banded spherulites in crystalline polylactides. Also, for comparison, the band spacing of the banded spherulites was determined in the blends of PLLA/PCL (Figure 2). Similar to the PS−PLLA, the band spacing increased with the increase of crystallization temperature. However, in contrast to the PS−PLLA, significant increase in the band spacing in PLLA/PCL blends was found. The difference implicitly indicates that the incompatible PS block chemically jointed with the PLLA block indeed plays an important role in the effect of diluents so as to give higher HTP in the lamellar twisting.

Now the question is whether the effect of chirality is the primary factor for the formation of banded spherulites or the effect of diluents. To justify the effects of chirality and diluents, ternary blends of PLLA, PDLA, and PCL were prepared. The approach is to prepare the blends of PLLA and PDLA at equimolar fraction so as to degenerate the chiral effect for the formation of the banded spherulites. Meanwhile, a compatible diluent, PCL, is introduced to the racemic blends so as to provide the effect of diluents. As shown in Figures 6a−d, no banded spherulites can be obtained under any crystallization conditions. We thus conclude that the effect of chirality for the induction of crystalline asymmetry is the primary factor for the formation of the banded spherulites, and the effect of diluents is an

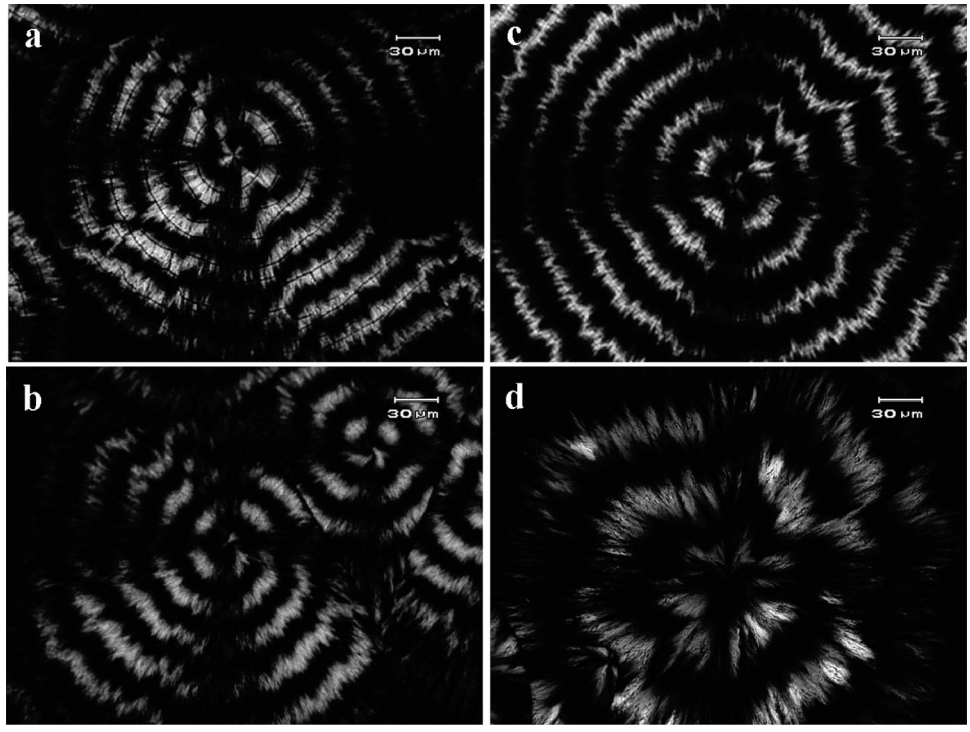

Figure 5. PLM morphologies of banded spherulites in the blends of PLLA and PCL homopolymers ($f_{PLLA}^{v} = 0.65$) crystallized from melt at different temperatures: (a) 110, (b) 115, (c) 120, and (d) 130 °C.

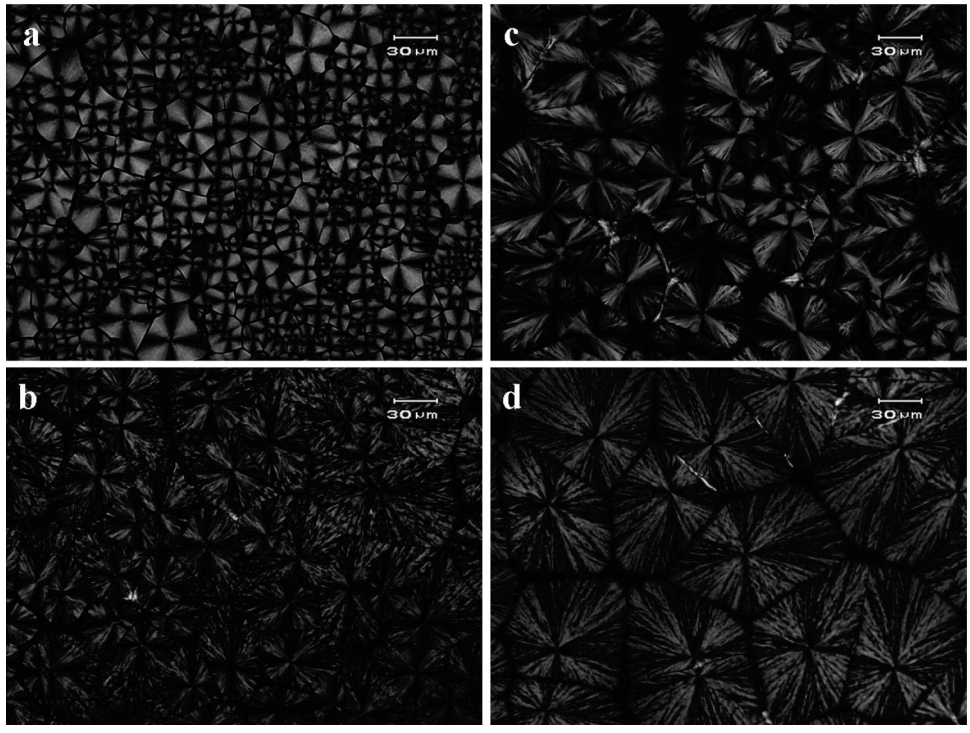

Figure 6. PLM morphologies of spherulites in the blends of PLLA, PDLA, and PCL with equimolar PLLA and PDLA (the volume fraction of polylactides in the blends is 0.65) crystallized from melt at different crystallization temperatures: (a) 130, (b) 140, (c) 150, and (d) 160 °C.

important factor to intensify the effect of chirality. Detailed mechanisms with respect to the crystalline growth of chiral polymers, in particular in the presence of compatible diluents, will be discussed below.

Crystalline Lamellar Morphologies in Spherulites. To further examine the crystalline lamellar morphologies in the banded spherulites, PS−PLLA thin-film samples were prepared and examined by TEM (Figure 7). As shown, crystalline lamellae helically grow from the center of spherulites and exhibit slightly wavy crystalline lamellar morphology. We speculate that the formation of the wavy morphology is attributed to the crystalline lamellar twisting; similar results can also be found in the banded spherulites of poly(trimethylene terephthalate) as observed in our laboratory previously.[2] By taking advantage of the degradable character of PLLA, hydrolyzed PS−PLLA thin-film samples were prepared so as to directly observe the growth profile of PLLA crystals at which the connected amorphous PS block can be removed with the hydrolyzed amorphous PLLA.

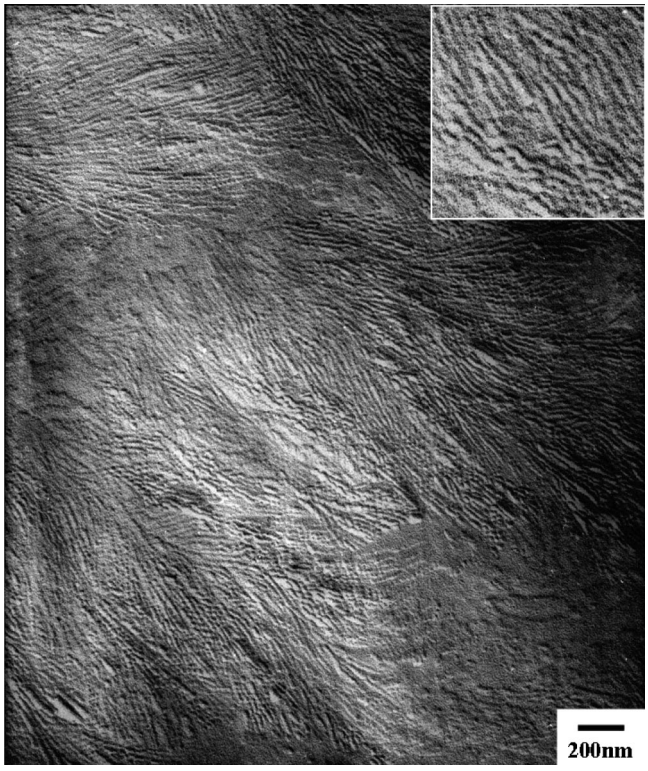

Figure 7. TEM micrograph of PS−PLLA banded spherulites crystallized from melt at 120 °C. The sample was shadowed by platinum. The inset shows the enlarged area.

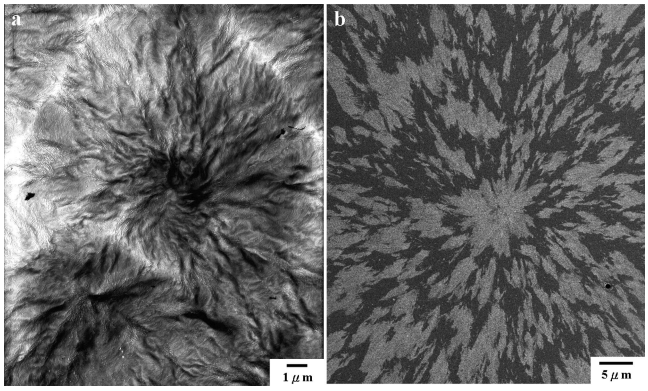

Figure 8. (a) TEM and (b) FESEM micrographs of PS−PLLA banded spherulites crystallized from melt at 120 °C. The samples were hydrolyzed first and then shadowed by Pt and sputtered with gold for TEM and FESEM, respectively.

As examined by TEM (Figure 8a), periodic variation in height can be recognized, and the periodic length of topographic variation is approximately equal to the pitch length of the banded texture observed by PLM. Similar results can also be observed by FESEM (Figure 8b). Those results are consistent with the hypothesis of the formation of alternating flat-to-edge-on morphology (namely, lamellar twisting) for the cause of extinction bands. To further examine the crystalline lamellar texture from the spherulites, high-magnification TEM micrographs for hydrolyzed PLLA and PS−PLLA samples were obtained. A straight crystalline lamellar fibrillar texture can be clearly identified in the PLLA (Figure 9a), whereas irregular PLLA crystalline lamellae were observed in the PS−PLLA (Figure 9b). We speculate that, in contrast to PLLA homopolymer, the irregular PLLA crystalline lamellae in the PS−PLLA might be attributed to the dangling PS chains that strongly

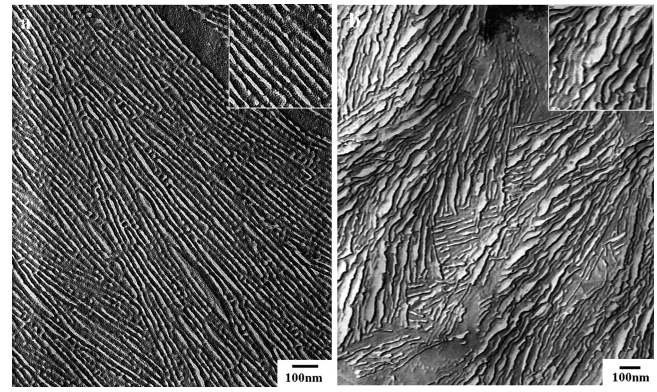

Figure 9. TEM micrographs of crystalline lamellar morphology crystallized from melt at 120 °C: (a) PLLA homopolymer; (b) PS−PLLA block copolymer. The samples were hydrolyzed first and then shadowed by Pt. The insets show the enlarged areas.

perturb the growth of PLLA crystalline lamellae during isothermal crystallization.

Origins for the Formation of Banded Texture in PS−PLLA. As mentioned, the origins for the formation of the banded spherulites remain an open question. It is generally believed that the occurrence of the extinction bands is attributed to the cooperative lamellar twisting along the radial direction for crystal growth. In the case of chiral polymers such as crystalline polylactides, the formation of the banded spherulites is referred to the effect of chirality. Also, as reported by Prud'homme and co-workers, lamellar curvature with exclusive direction can be obtained in the crystalline polylactides,[25] suggesting that the formation of twist lamellae for crystalline polylactides. Moreover, in contrast to polylactide homopolymers, the formation of the banded spherulites can be much easily obtained in the PS−PLLA. As a result, we suggest that the chiral effect is necessary for the induction of the cooperative lamellar twisting in the radial growth direction so as to result in the banded spherulites in PLM. Furthermore, the chiral effect is enhanced by the introduction of diluents, such as compatible PCL homopolymer, that promotes the formation of the banded spherulites; this is referred to as the diluent effect. Therefore, a hypothetical mechanism for the formation cooperative lamellar twisting in the PS−PLLA is proposed as illustrated in Figure 10. The PLLA chains first crystallize to form crystalline lamella ($PLLA^c$). However, on the basis of the two-phase model for crystalline polymers, there should remain amorphous PLLA chains ($PLLA^a$), illustrated as a helical shape in Figure 10. Also, dangling amorphous PS chains appear as a random coiled conformation, illustrated as an elliptical shape in Figure 10. According to the mechanism proposed by Keith and Padden, the chain folding, steric hindrance, or chain tilt could result in the curvature of polymer crystals.[17,43,44] In the case of crystalline polylactides, Prud'homme and co-workers also verified that there would be an imbalanced surface stress at crystalline lamellar fold surfaces due to the different rotational sense of helical chains for chain folding so as to lead to the crystalline lamellar curvature.[25] Therefore, an imbalanced surface stress at the fold surfaces should also be expected in the PS−PLLA. As illustrated, the imbalanced surface stress is initiated from the lamellar fold surface due to the effect of chirality that is the primary factor to cause the crystalline lamella twist. In addition, the imbalanced surface stress is intensified by the effect of diluents due to the existence of dangling amorphous PLLA and PS chains. In particular, the elliptical PS random coiled chains, dangling from the PLLA crystalline lamella surface via chemical junction, can be regarded as the origin for the amplification of steric hindrance effect (i.e., the effect of chirality) due to the

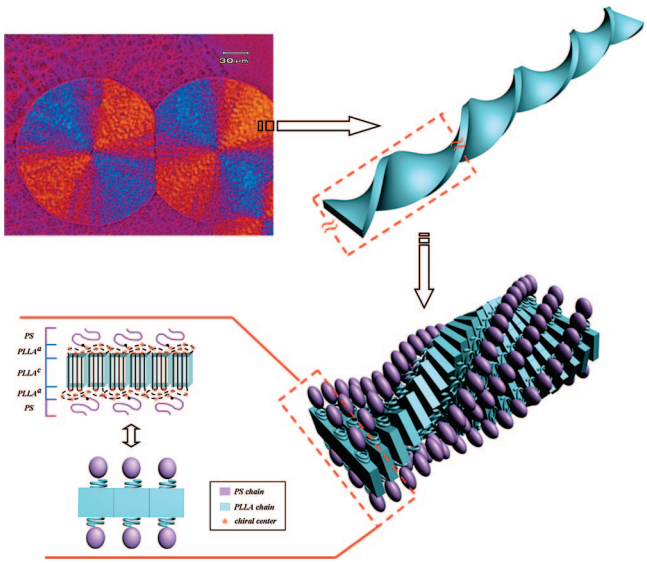

Figure 10. Illustration of crystalline lamellar twisting in PS−PLLA banded crystalline spherulites with negative birefringence character. The observed crystalline lamellar twisting arises from imbalanced surface stress at crystalline lamellar fold surfaces due to the different rotational sense of chiral PLLA chains. In addition, the imbalanced surface stress is intensified by the effect of diluents due to the existence of dangling amorphous PLLA and PS chains. Consequently, the imbalanced surface stress cooperatively drives the crystalline lamellar twisting and finally leads to the formation of banded texture.

formation of phase separation resulting from incompatibility. As a result, the twisting of the crystalline lamellae would be enhanced by increasing the separation of the PS coils in order to relieve the surface stress for lower Gibbs free energy state (that is, more stable state). As demonstrated, the twisting indeed affects the average separation between the joints of the PS and PLLA blocks. Consequently, the effect of the steric hindrance that causes imbalanced surface stress intensified by the presence of the PS block leads to significant crystalline lamellar twisting so as to result in the banded spherulites with higher HTP (namely, smaller band spacing).

Conclusions

A banded spherulite with negative birefringence character was observed in crystalline PS−PLLA thin films by PLM. In contrast to typical spherulite in neat PLLA homopolymer, we suggest that the appearance of the banded spherulites is attributed to the imbalanced surface stress at the fold surfaces for the lamellar twisting that can be intensified by the PS block due to the effect of diluents on the formation of the banded spherulites in chiral PLLA crystalline lamellar. This hypothesis was justified by examining different blending systems, in particular a racemic blend. As demonstrated, the chirality of PLLA is the primary factor for the induction of cooperative lamellar twisting along the radial growth direction to form banded spherulites, and compatible diluents are an important factor to intensify the chiral effect. In the PS−PLLA, the imbalanced surface stress is intensified by the existence of dangling amorphous PS chains that significantly enhance the effect of diluents so as to result in high twisting power of twist lamellae (namely, decrease in the band spacing of spherulites). The mechanism for the morphological evolution of banded spherulites in crystalline PS−PLLA may provide further understanding for the formation of the banded spherulites in chiral polymeric materials.

Acknowledgment. This research was supported by the National Science Council (NSC) of Taiwan NSC95-2221-E007-131-MY2. Our appreciation is extended to Ms. P.-C. Chao and Mr. Y.-F. Lu of Regional Instruments Center at NCHU for their help in TEM and FESEM experiments, respectively.

References and Notes

(1) Keith, H. D.; Padden, F. J., Jr.; Russell, T. P. *Macromolecules* **1989**, *22*, 666–675.
(2) Ho, R.-M.; Ke, K.-Z.; Chen, M. *Macromolecules* **2000**, *33*, 7529–7537.
(3) Xu, J.; Guo, B.-H.; Zhang, Z.-M.; Zhou, J.-J.; Jiang, Y.; Yan, S.; Li, L.; Wu, Q.; Chen, G.-Q.; Schultz, J. M. *Macromolecules* **2004**, *37*, 4118–4123.
(4) Shin, D.; Shin, K.; Aamer, K. A.; Tew, G. N.; Russell, T. P.; Lee, J. H.; Jho, J. Y. *Macromolecules* **2005**, *38*, 104–109.
(5) Keller, A. *J. Polym. Sci.* **1955**, *17*, 351–364.
(6) Keith, H. D.; Padden, F. J., Jr *J. Polym. Sci.* **1959**, *39*, 101–122.
(7) Keith, H. D.; Padden, F. J., Jr *J. Polym. Sci.* **1959**, *39*, 123–138.
(8) Price, F. P. *J. Polym. Sci.* **1959**, *39*, 139–150.
(9) Keller, A. J. *Polym. Sci.* **1959**, *39*, 151–173.
(10) Fujiwara, Y. J. *Appl. Polym. Sci.* **1960**, *4*, 10–15.
(11) Schultz, J. M.; Kinloch, D. R. *Polymer* **1969**, *10*, 271–278.
(12) Schultz, J. M. *Polymer* **2003**, *44*, 433–441.
(13) Bassett, D. C.; Hodge, A. M. *Polymer* **1978**, *19*, 469–472.
(14) Bassett, D. C.; Vaughan, A. S. *Polymer* **1985**, *26*, 717–725.
(15) Bassett, D. C.; Olley, R. H.; Al-Raheil, A. M. *Polymer* **1988**, *29*, 1539–1543.
(16) Keller, A. *J. Polym. Sci.* **1955**, *17*, 291–308.
(17) Keith, H. D.; Padden, F. J., Jr *Polymer* **1984**, *25*, 28–42.
(18) Lustiger, A.; Lotz, B.; Duff, T. S. *J. Polym. Sci., Polym. Phys. Ed.* **1989**, *27*, 561–579.
(19) Singfield, K. L.; Klass, J. M.; Brown, G. R. *Macromolecules* **1995**, *28*, 8006–8015.
(20) Lotz, B.; Cheng, S. Z. D. *Polymer* **2005**, *46*, 577–610.
(21) Li, C. Y.; Cheng, S. Z. D.; Ge, J. J.; Bai, F.; Zhang, J. Z.; Mann, I. K.; Chien, L. C.; Harris, F. W.; Lotz, B. *J. Am. Chem. Soc.* **2000**, *122*, 72–79.
(22) Li, C. Y.; Cheng, S. Z. D.; Weng, X.; Ge, J. J.; Bai, F.; Zhang, J. Z.; Calhoun, B. H.; Harris, F. W.; Chien, L. C.; Lotz, B. *J. Am. Chem. Soc.* **2001**, *123*, 2462–2463.
(23) Singfield, K. L.; Hobbs, J. K.; Keller, A. *J. Cryst. Growth* **1998**, *183*, 683–689.
(24) Xu, J.; Guo, B.-H.; Zhou, J.-J.; Li, L.; Wu, J.; Kowalczuk, M. *Polymer* **2005**, *46*, 9176–9185.
(25) Maillard, D.; Prud'homme, R. E. *Macromolecules* **2006**, *39*, 4272–4275.
(26) Quiram, D. J.; Register, R. A.; Marchand, G. R.; Adamson, D. H. *Macromolecules* **1998**, *31*, 4891–4898.
(27) Zhu, L.; Cheng, S. Z. D.; Calhoun, B. H.; Ge, G.; Quirk, R. P.; Thomas, E. L.; Hsiao, B. S.; Yeh, F.; Lotz, B. *J. Am. Chem. Soc.* **2000**, *122*, 5957–5967.
(28) Zhu, L.; Cheng, S. Z. D.; Calhoun, B. H.; Ge, G.; Quirk, R. P.; Thomas, E. L.; Hsiao, B. S.; Yeh, F.; Lotz, B. *Polymer* **2001**, *42*, 5829–5839.
(29) Zhu, L.; Huang, P.; Chen, W. Y.; Ge, Q.; Quirk, R. P.; Cheng, S. Z. D.; Thomas, E. L.; Lotz, B.; Hsiao, B. S.; Yeh, F.; Lin, L. *Macromolecules* **2002**, *35*, 3553–3562.
(30) Ho, R.-M.; Lin, F.-H.; Tsai, C.-C.; Lin, C.-C.; Ko, B.-T.; Hsiao, B. S.; Sics, I. *Macromolecules* **2004**, *37*, 5985–5994.
(31) Ho, R.-M.; Chung, T.-M.; Tsai, J.-C.; Kuo, J.-C.; Hsiao, B. S.; Sics, I. *Macromol. Rapid Commun.* **2005**, *26*, 107–111.
(32) Chen, H.-L.; Hsiao, S.-C.; Lin, T.-L.; Yamauchi, K.; Hasegawa, H.; Hashimoto, T. *Macromolecules* **2001**, *34*, 671–674.
(33) Ho, R.-M.; Chiang, Y.-W.; Tsai, C.-C.; Lin, C.-C.; Ko, B.-T.; Huang, B.-H. *J. Am. Chem. Soc.* **2004**, *126*, 2704–2705.
(34) Chiang, Y.-W.; Ho, R.-M.; Ko, B.-T.; Lin, C.-C. *Angew. Chem., Int. Ed.* **2005**, *44*, 7969–7972.
(35) Ho, R.-M.; Chen, C.-K.; Chiang, Y.-W.; Ko, B.-T.; Lin, C.-C. *Adv. Mater.* **2006**, *18*, 2355–2358.
(36) Zalusky, A. S.; Olayo-Valles, R.; Taylor, C. J.; Hillmyer, M. A. *J. Am. Chem. Soc.* **2001**, *123*, 1519–1520.
(37) Ho, R.-M.; Tseng, W.-H.; Fan, H.-W.; Chiang, Y.-W.; Lin, C.-C.; Ko, B.-T.; Huang, B.-H. *Polymer* **2005**, *46*, 9362–9377.
(38) Zalusky, A. S.; Olayo-Valles, R.; Wolf, J. H.; Hillmyer, M. A. *J. Am. Chem. Soc.* **2002**, *124*, 12761–12773.
(39) Tsuji, H.; Tezuka, Y. *Biomacromolecules* **2004**, *5*, 1181–1186.
(40) Tsuji, H.; Ikada, Y. *Macromolecules* **1993**, *26*, 6918–6926.
(41) Ho, R.-M.; Hsieh, P.-Y.; Tseng, W.-H.; Lin, C.-C.; Huang, B.-H.; Lotz, B. *Macromolecules* **2003**, *36*, 9085–9092.
(42) Hamley, I. W.; Castelletto, V.; Castillo, R. V.; Muller, A. J.; Martin, C. M.; Pollet, E.; Dubois, Ph. *Macromolecules* **2005**, *38*, 463–472.
(43) Keith, H. D.; Padden, F. J., Jr *Macromolecules* **1996**, *29*, 7776–7786.
(44) Lovinger, A. J.; Keith, H. D. *Macromolecules* **1996**, *29*, 8541–8542.

MA702416N